

Dear ACP Editor

After carefully reading the comments from the two reviewers, we have revised our manuscript. Following is our response to the comments.

Anything about our paper, please feel free to contact me via [wanggh@ieecas.cn](mailto:wanggh@ieecas.cn)

Sincerely yours

Gehui Wang  
2016-11-25

### **Referee No. #1**

#### **General comments:**

The study compared the PM before, during and after APEC in 2014. The study focused on organic compounds in fine particles and they understand how these organic compounds change during the emission control. Recently, many previous studies prove the organics in fine particles were dominant in North China plain which could be important policy to control VOCs in the future. However, details about organic compounds is scare. Obviously, the study is important to provide more details about organics. Moreover, during the APEC period, the Chinese central government made strick emission control in North China Plain in winter. After the APEC period, one severe haze-fog event occurred. The phenonmon provides one change to understand what kind of chemical mechanism to promote the haze formation following the source emission change. I think the study provide some insights to improve the air quality in Beijing and well understand details about organics. After the reading, the current ms need to be revised after one publication.

**Response:** We thank the reviewer' comments above and revised our manuscript. Following is our detailed response to the comments

#### **Comments**

(1) Abstract: The abstract is so long and two paragraph. I may suggest to take some details away and make major findings in the abstract.

**Response:** Suggestion taken. We have shortened the abstract by removing some details. See page 2, line 42-60.

#### **Comments**

(2) Title: Molecular distributions” what does this mean? I think the authors only provide the concentration changes of oxalic acid and related SOA. Seemly, the word is not correct here.

**Response:** We changed the title as “Concentrations and stable carbon isotope compositions of oxalic acid and related SOA in Beijing before, during and after the 2014 APEC event”

### **Comments**

(3) L253-254, the statement is unexpected. Could you show the result in anywhere? Also, the data only containing  $\text{NH}_4^+$  as the basic ion is bias. What about  $\text{Na}^+$ ,  $\text{K}^+$ , and  $\text{Ca}^{2+}$ ? I think the bisulfate depending on the particle size. More smaller particle size is more acidic. Therefore, the conclusion should be revised. Also, I noticed several pervious papers in ACP. They found the Beijing air is  $\text{NH}_3$ -rich not  $\text{NH}_3$ -limited. Please find them and carefully made the conclusion.

**Response:** We are sorry that we did not give the related information in the ACPD version. The fact is that we have measured all cations and anions in the samples and input these data into ISORRPIA-II mode, which has treated the  $\text{Na}^+$ - $\text{NH}_4^+$ - $\text{K}^+$ - $\text{Ca}^{2+}$ - $\text{Mg}^{2+}$ - $\text{Cl}^-$ - $\text{NO}_3^-$ - $\text{SO}_4^{2-}$  system, to estimate the aerosols liquid water content (ALWC) and acidity ( $[\text{H}^+_{\text{aero}}]$ ). We agree with the reviewer that Beijing air is not  $\text{NH}_3$ -limited, because we found that the molar ratio of  $\text{NH}_4^+$  to  $\text{SO}_4^{2-}$  plus  $\text{NO}_3^-$  is 1.1 for the current work, which means that sulfate and nitrate in Beijing during the APEC campaign were completely neutralized. Such a conclusion is consistent with our work about Beijing haze published in PNAS recently (Wang et al., 2016). Weber et al (2016) reported that under the typical rural conditions over southeastern USA for ammonium sulfate aqueous particles the equilibrium  $\text{NH}_3$  vapor concentrations is approximately  $160 \mu\text{g m}^{-3}$  (220 ppbv), which is far beyond the real concentration of  $\text{NH}_3$  in the atmosphere and means that ammonium bisulfate is the major form of sulfate existing in the atmosphere under a typical ambient level of  $\text{NH}_3$  conditions.

In the revised version, one paragraph and related data about the model calculation has been added into the text, see page 6, line 131-135 and page 22, Table 1. We also polished the statements related to aerosol acidity, see page 11, line 241-245.

### **Comments:**

(4) Section 3.3.2 Figure 6 shows three classes of air masses. I am confused the name of the type. I think the regional type is same to long-range transport type. Also, Local type is not local from the Figure 6. Obviously, the name should be modified. I suggest that long-range transport type should be clean air mass. Regional type should be polluted air mass. Local type should be mixed type of clean and polluted.

**Response:** Suggestion taken. In the current version, we re-named the three types of air masses as polluted, clean and mixed, as recommended by the reviewer, and revised all the related discussions. See Section 3.3.2 and Figure 6.

### **Comments:**

(5) L269-271 and L339-341 the result is not stable for temperature. The  $\text{PM}_{2.5}$  decrease is associated with air masses or wind direction. If the air mass was from northwest, the  $\text{PM}_{2.5}$  concentration decreased because it bring the clean air into Beijing. Also the temperature is decrease. As it is, you can make conclusion about the  $\text{PM}_{2.5}$  concentration and oxalic formation? If the authors want to make such conclusion, you need to compare the  $\text{PM}_{2.5}$  and oxalic concentration at similar air masses such both from south.

**Response:** We agree with the reviewer that the much less abundant  $\text{PM}_{2.5}$  and oxalic acid during-APEC is related to the air masses, which originated from Siberia and Mongolia and

brought clean air into Beijing. We looked at the correlation of  $C_2/TDOC$  with temperature for each type of air masses, and found the correlation still exists and even more significant, for example, the  $R^2$  is 0.56 and 0.67 for the polluted type of air masses and the clean type of air masses, respectively, which indicates that higher temperature conditions are favorable for oxidation of precursors to produce oxalic acid. We have revised the related discussions. See page 10, line 251-258.

For the conclusion in previous version, i.e., L339-341, we have deleted these sentences in the current revised paper, because we believe the original version of statement overemphasized the importance of temperature in for  $PM_{2.5}$  reduction and thus is not accurate enough. The lower  $PM_{2.5}$  and SOA concentrations during-APEC period are not only due to the efficient emission controls but also due to the favorable meteorological conditions. During the APEC period air masses arriving in Beijing mostly originated from Siberia and Mongolia, which are clean, cold, and relatively drier compared with those before-APEC. Thus,  $PM_{2.5}$  and oxalic acid concentrations are much lower. See the revised sentences in page 15, line 328-335, and line 351-357.

### **Comments:**

In the context, the authors miss comma before and. Such L50 before-, during-, and after-APEC.

L216 L319,  $SO_4^{2-}$ ,  $NO_3^-$ ,  $NH_4^+$ .

L293 North

L294 is – was

L341 not only, but also changed to by both the emission controls and the lower tem.;

**Response:** Suggestion taken. We have corrected these. See page 12, line 281-282 and page 14, line 308.

## **Referee #2**

### **General comments:**

This manuscript investigates aerosol chemical compositions before, during and after the APEC event. The authors also provide some valuable measurement data, e.g., particulate organic matters on molecular level and isotope compositions, to testify the effect of emission reduction, temperature and RH on secondary aerosol formation. Overall, this paper is definitely of interest for the scientific community and the findings are relevant to a better understanding the influence of pollution control on atmospheric aerosols. However, some revision work as listed below should be done before publication could be considered.

**Response:** We thank the reviewer' comments above and revised our manuscript. Following is our detailed response to the comments

### **General comments:**

The authors try to ascribe the low concentration of and relative abundances of SIA, WSOC, TDOC and C<sub>2</sub> during and after APEC to the low temperature condition. However, as shown in figure 6 in the manuscript, the backward trajectory cluster analysis demonstrates that there are more stagnant air masses before APEC than those during APEC, and "...the resident time of the air masses within Hebei province is very short, thus aerosols...is of local characteristics and relatively fresh". This is self-contradictory. If the backward trajectory cluster analysis is right, all the secondary features before APEC can be ascribed to the more time for the formation of secondary aerosols, instead of high temperature which favor the secondary formation. The authors need to clarify this contradiction.

**Response:** Suggestion taken. We agree with the reviewer that reaction time, in addition to temperature, is also important for secondary aerosol formation, i.e., the stagnant condition before-APEC is favorable for secondary aerosol formation. However, we do not think all the secondary features before APEC should be ascribed to the more time for the formation of secondary aerosols, because temperature and relative humidity are also important factors for photochemical oxidation especially for aerosol aqueous phase oxidation. Higher temperatures and humid conditions are favorable for SOA aqueous-phase production, which could result in abundant oxalic acid enriched with heavier <sup>13</sup>C (Aggarwal and Kawamura, 2008; Wang et al., 2012). In the current revised version, we have modified all the related explanations about the lower concentrations and relative abundances of SIA, WSOC, TDOC and C<sub>2</sub> during- and after-APEC throughout the paper including abstract.

### **Comments:**

1. Line 232, "In comparison with those before-APEC the decreased ratio C<sub>2</sub>/TDOC and increased ratios of Gly/TDOC and mGly/TDOC during and after-APEC, together with a decreased ratio of WSOC/OC discussed previously, further suggest a reducing production of SOA during the whole campaign." This sentence is very obscure.

**Response:** We have modified this statement. See page 10, line 218-223.

### **Comments:**

2. Line 254, "As seen in Fig. 5d, H+aer correlated well with SO<sub>4</sub><sup>2-</sup> (R<sub>2</sub> = 0.58), probably suggesting SO<sub>4</sub><sup>2-</sup> is the key factor controlling the aerosol acidity." The logic of this sentence is questionable. The acidity of aerosols is decided by the anion-cation balance, not a single ion.

**Response:** We agree with the reviewer that the acidity of aerosols is decided by the anion-cation balance, not a single ion. The fact is that we determined all cations and anions in the samples not a single ion, and put these data into ISORROPIA-II model, which treated the Na<sup>+</sup>-NH<sub>4</sub><sup>+</sup>-K<sup>+</sup>-Ca<sup>2+</sup>-Mg<sup>2+</sup>-Cl<sup>-</sup>-NO<sub>3</sub><sup>-</sup>-SO<sub>4</sub><sup>2-</sup> system, to estimate the aerosol aqueous H<sup>+</sup> concentration (Hennigan et al, 2015; Weber et al., 2016). We revised this sentence to make the explanation more reasonable. See page 11, line 241-245.

### **Comments:**

3. Line 262, as discussed above, good correlation between the temperature and C<sub>2</sub>/TDOC may because the different origin of air mass.

**Response:** We have looked at the correlation for the different air masses, and found the linear correlation still exists and is even more significant. For example, the linear correlation coefficients are  $R^2=0.56$  for the polluted type of air masses and  $R^2=0.67$  for the clean type of air masses, further demonstrating that temperature is an important factor for organic aerosol oxidation, i.e., higher temperature is favorable for organic aerosol oxidation. We have modified these discussions. See page 10-11, line 251-258.

**Comments:**

4. Line 279, is it possible that the change of  $\delta^{13}\text{C}$  in  $\text{C}_2$  is due to the different source of  $\text{C}_2$  precursors?

**Response:** We do not think so. Oxalic acid ( $\text{C}_2$ ) in the atmosphere mostly exists in aerosol phase and is produced via aerosol-phase oxidation of organic compounds with two or more carbon atoms. Changes in  $\delta^{13}\text{C}$  of atmospheric  $\text{C}_2$  is caused by stable carbon isotope fractionation process, which occurs during the  $\text{C}_2$  precursor oxidation process and called as kinetic isotope effects (KIE), rather than by the different source of  $\text{C}_2$  precursors (Kawamura et al., 2016, Hoefs 2009). Many studies have found that oxalic acid is enriched with heavier  $^{13}\text{C}$  during aerosol ageing process, thus  $\delta^{13}\text{C}$  of  $\text{C}_2$  often displays a positive correlation with its relative abundance. Because during aerosol ageing process organic aerosols release  $\text{CO}_2/\text{CO}$  by reaction with OH radical and other oxidants, resulting in the evolved species enriched with lighter isotope ( $^{12}\text{C}$ ) and the remaining substrate enriched in  $^{13}\text{C}$  due to KIE effects (Hoefs, 1997; Rudolph et al., 2002).

**Comments**

5. Line 288, I am a little confused about the definition of the pollution type. Do the authors find higher relative concentration of primary pollutant, e.g., BC, CO, in the local type? Also, the air masses from Siberia should be very clean. Is there any evidence of the pollutant transport during the periods of this type? Otherwise, the use of “transport” in the definition will be misleading.

**Response:** In the revised paper we have re-named the three types of air masses, as recommended by the reviewer #1. Yes, we found higher relative concentration of primary pollutant (e.g., BC and CO) in the local type (now is re-named as the mixed type). Higher relative abundances of primary species were observed for the  $\text{PM}_{2.5}$  samples collected after-APEC, for example, EC/ $\text{PM}_{2.5}$  is 3% in the event I and increased to 7.5% in the event II. We have added this into the text. See page 14, line 324-327.

Long-range transport is a commonly used term by aerosol researchers when they talk about aerosol origins. There is a certain amount of natural organic aerosols in the atmosphere over Siberia and Mongolia, although their concentrations are much lower compared to the anthropogenic aerosols in the downwind regions such as Beijing. During the moving of air masses from Siberia and Mongolia to east China, these particles can be transported. However, as recommended by the reviewer #1, we re-defined the three types of air masses and revised related statements to avoid any possible misleading. See page 12-13, line 273-303.

**Comments:**

6. Line 308, still, is it possible that the difference of  $\delta^{13}\text{C}$  in each type is due the different

source of C<sub>2</sub> precursors?

**Response:** We don't think so. See our response above.

**Comments:**

7. Line 315, the authors compared two pollutant episodes before and after APEC, and conclude that the difference is mainly due to the temperature. However, as it is also discussed in Part 3.3.2, the two episodes are in different pollution types with totally different air mass origin. The authors need to exclude the influence of air mass before making such conclusions.

**Response:** We think in the ACPD version we overemphasized the role of temperature and neglected other factors such as stagnant condition that caused a longer reaction time before-APEC for SOA formation. Thus our conclusion that the difference before- and after-APEC is mainly due to the temperature is not accurate enough. We have revised our explanation about the aerosol composition difference. See page 14, line 309-313; page 14-15, line 324-335.

Reference

- Aggarwal, S.G., and Kawamura, K. Molecular distributions and stable carbon isotopic compositions of dicarboxylic acids and related compounds in aerosols from Sapporo, Japan: implications for photochemical aging during long-range atmospheric transport. *J. Geophys. Res. Atmos.* 113, D14301, 2008.  
<http://dx.doi.org/10.1029/2007JD009365>.
- Hennigan, C. J., Izumi, J., Sullivan, A. P., Weber, R. J., and Nenes, A.: A critical evaluation of proxy methods used to estimate the acidity of atmospheric particles, *Atmos. Chem. Phys.*, 15(5), 2775-2790, 2015.
- Hoefs, J. (1997), *Stable Isotope Geochemistry.*, Springer, New York.
- Kawamura, K., and Bikkina, S.: A review of dicarboxylic acids and related compounds in atmospheric aerosols: Molecular distributions, sources and transformation, *Atmospheric Research*, 170, 140-160, 2016.
- Rudolph, J., Czuba, E., Norman, A., Huang, L., and Ernst, D.: Stable carbon isotope composition of nonmethane hydrocarbons in emissions from transportation related sources and atmospheric observations in an urban atmosphere, *Atmos. Environ.*, 36, 1173-1181, 2002.
- Wang, G., Kawamura, K., Cao, J., Zhang, R., Cheng, C., Li, J., Zhang, T., Liu, S., and Zhao, Z.: Molecular distribution and stable carbon isotopic composition of dicarboxylic acids, ketocarboxylic acids and -dicarbonyls in size-resolved atmospheric particles from Xi'an city, China, *Environ. Sci. Technol.*, 46, 4783-4791, 2012.
- Wang, G., Zhang, R., Zamora, M. L., Gomez, M. E., Yang, L., Hu, M., Lin, Y., Guo, S., Meng, J., Li, J., Cheng, C., Hu, T., Ren, Y., Wang, Y., Gao, J., Cao, J., An, Z., Zhou, W., Jiayuan Wang, Marrero-Ortiz, W., Tian, P., Secretst, J., Peng, J., Du, Z., Jing Zheng, Shang, D., Zeng, L., Shao, M., Wang, W., Huang, Y., Wang, Y., Zhu, Y., Li, Y., Hu, J., Pan, B., Cai, L., Cheng, Y., Rosenfeld, D., Liss, P. S., Duce, R. A., Kolb, C. E., and Molina, M. J.: Persistent Sulfate Formation from London Fog to Chinese Haze, *Proceedings of National Academy of Science of United States of America*, doi/10.1073/pnas.1616540113., 2016.
- Weber, R. J., Guo, H., Russell, A. G., and Nenes, A.: High aerosol acidity despite declining atmospheric sulfate concentrations over the past 15 years, *Nature Geoscience*, doi:10.1038/NGEO2665, 2016.

1 **Concentrations** and stable carbon isotope compositions of oxalic  
2 acid and related SOA in Beijing before, during and after the  
3 2014 APEC  
4  
5  
6  
7  
8  
9

10 Jiayuan Wang<sup>1,3</sup>, Gehui Wang<sup>1,2,3,4,\*</sup>, Jian Gao<sup>5,6,\*</sup>, Han Wang<sup>5,6</sup>, Yanqin Ren<sup>1,3</sup>,  
11 Jianjun Li<sup>1</sup>, Bianhong Zhou<sup>1</sup>, Can Wu<sup>1,3</sup>, Lu Zhang<sup>1,3</sup>, Shulan Wang<sup>5,6</sup>, Fafe Chai<sup>5,6</sup>  
12  
13  
14  
15  
16  
17  
18  
19  
20  
21

22 <sup>1</sup>State Key Laboratory of Loess and Quaternary Geology, Key Lab of Aerosol Chemistry and  
23 Physics, Institute of Earth Environment, Chinese Academy of Sciences, Xi'an 710061, China

24 <sup>2</sup>School of Human Settlements and Civil Engineering, Xi'an Jiaotong University, Xi'an 710079,  
25 China

26 <sup>3</sup>University of Chinese Academy of Sciences, Beijing 100049, China

27 <sup>4</sup>Center for Excellence in Regional Atmospheric Environment, Institute of Urban Environment,  
28 Chinese Academy of Sciences, Xiamen 361021, China

29 <sup>5</sup>State Key Laboratory of Environmental Criteria and Risk Assessment, Chinese Research  
30 Academy of Environmental Sciences, Beijing 100084, China

31 <sup>6</sup>Collaborative Innovation Center of Atmospheric Environment and Equipment Technology,  
32 Nanjing 210000, China  
33  
34  
35  
36

37 *Correspondence to:* Gehui Wang ([wanggh@ieecas.cn](mailto:wanggh@ieecas.cn)) and Jian Gao ([gaojian@craes.org.cn](mailto:gaojian@craes.org.cn))  
38  
39  
40  
41

42 **Abstract:** To ensure the good air quality for the 2014 APEC, stringent emission controls were  
43 implemented in Beijing and its surrounding regions, leading to a significant reduction in PM<sub>2.5</sub>  
44 loadings. To investigate the impacts of the emission controls on aerosol composition and  
45 formation, high-volume PM<sub>2.5</sub> samples were collected in Beijing from 8<sup>th</sup> October to 24<sup>th</sup>  
46 November, 2014 and determined for secondary inorganic ions (SIA, i.e., SO<sub>4</sub><sup>2-</sup>, NO<sub>3</sub><sup>-</sup> and NH<sub>4</sub><sup>+</sup>),  
47 dicarboxylic acids, keto-carboxylic acid and  $\alpha$ -dicarbonyls, as well as stable carbon isotope  
48 composition of oxalic acid (C<sub>2</sub>). Our results showed that SIA, C<sub>2</sub> and related SOA in PM<sub>2.5</sub>  
49 before-APEC were 2–4 times higher than those during-APEC, which can be ascribed to the  
50 warm, humid and stagnant conditions before-APEC that are favorable for secondary aerosol  
51 production.

52 C<sub>2</sub> in the polluted air masses, which mostly occurred before-APEC, are abundant and  
53 enriched in <sup>13</sup>C. On the contrary, C<sub>2</sub> in the clean air masses, which mostly occurred during-APEC,  
54 is much less abundant but still enriched in <sup>13</sup>C. In the mixed type of clean and polluted air  
55 masses, which mostly occurred after-APEC, C<sub>2</sub> is lower than that before-APEC but higher than  
56 that during-APEC and enriched in lighter <sup>12</sup>C. A comparison on chemical composition of fine  
57 particles and  $\delta^{13}\text{C}$  values of C<sub>2</sub> in two events that are characterized by high loadings of PM<sub>2.5</sub>  
58 further showed that after-APEC SIA and TDOC are much less abundant and fine aerosols are  
59 enriched with primary organics and relatively fresh, compared with those before-APEC.

60

61 **Key words:** Secondary organic aerosols; Emission controls; Sources and formation mechanisms;  
62 Aqueous-phase oxidation; Aerosol acidity and water content.



63 **1. Introduction**

64 Atmospheric aerosols profoundly impact the global climate directly by scattering and  
65 absorbing solar radiation and indirectly by affecting cloud formation and distribution via acting  
66 as cloud condensation nuclei (CCN) and ice nuclei (IN). Moreover, atmospheric aerosols exert  
67 negative effects on human health because of their toxicity. Due to fast urbanization and  
68 industrialization, high level of atmospheric fine particle (PM<sub>2.5</sub>) pollution has been a persistent  
69 problem in many cities of China since the nineties of last century (van Donkelaar et al., 2010).  
70 As the capital of China and one of the largest megacities in the world, Beijing has suffered from  
71 frequent severe haze pollution especially in winter, affecting more than 21 million people by the  
72 end of 2014 (Beijing Municipal Bureau of Statistics, 2015) and causing billions of economic  
73 losses (Mu and Zhang, 2013). To improve the air quality Beijing government has put many efforts  
74 to reduce the pollutant emissions (i.e., SO<sub>2</sub>, NO<sub>x</sub>, dust, and volatile organic compounds (VOCs))  
75 from a variety of sources.

76 The 2014 Asia-Pacific Economic Cooperation (APEC) summit was hosted in Beijing from  
77 the 5<sup>th</sup> to 11<sup>th</sup> November. To ensure good air quality for the summit, a joint strict emission control  
78 program was conducted from 3<sup>rd</sup> November 2014 in Beijing and its neighboring provinces  
79 including Inner Mongolia, Shanxi, Hebei and Shandong provinces. During this period thousands  
80 of factories and power plants with high emissions were shut down and/or halted, all the  
81 construction activities were stopped and the numbers of on-road vehicles were reduced. These  
82 strict emission controls resulted in the air quality of Beijing during the APEC period being  
83 significantly improved, leading to a decrease in PM<sub>2.5</sub> concentration by 59.2% and an increase in  
84 visibility by 70.2% in Beijing during the summit compared with those before the APEC (Tang et

85 al., 2015) and a term of “APEC-Blue” being created to refer to the good air quality. Such strong  
86 artificial intervening not only reduced PM<sub>2.5</sub> and its precursors’ loadings in Beijing and its  
87 surrounding areas but also affected the composition and formation mechanisms of the fine  
88 particles (Sun et al., 2016).

89 A number of field measurements have showed that particle compositions in Beijing during  
90 wintertime haze periods are dominated by secondary aerosols (Guo et a., 2014; Huang et al,  
91 2014; Xu et al., 2015). Rapid accumulation of particle mass in Beijing during haze formation  
92 process is often accompanied by continuous particle size growth (Guo et al, 2014; Zhang et al.,  
93 2015), which is in part due to the coating of secondary organic aerosols (SOA) on pre-existing  
94 particles (Li et al., 2010). Several studies have found that SOA production during the 2014  
95 Beijing APEC periods significantly reduced and ascribed this reduction to the efficient regional  
96 emission control (Sun et al., 2016; Xu et al, 2015). However, up to now information of the SOA  
97 decrease on a molecular level has not been reported. Dicarboxylic acids are the major class of  
98 SOA species in the atmosphere and ubiquitously found from the ground surface to the free  
99 troposphere (Fu et al., 2008; Myriokefalitakis et al., 2011; Sorooshian et al., 2007; Sullivan et al.,  
100 2007). In the current work we measured molecular distributions of dicarboxylic acids,  
101 keto-carboxylic acids and  $\alpha$ -dicarbonyls and stable carbon isotope composition of oxalic acid in  
102 PM<sub>2.5</sub> aerosols collected in Beijing before, during and after the APEC event in order to explore  
103 the impact of the APEC emission control on SOA in Beijing. We first investigated the changes in  
104 concentration and composition of dicarboxylic acids and related compounds during the three  
105 periods, then recognized the difference in stable carbon isotope composition of oxalic acid in  
106 different air masses in Beijing during the APEC campaign. Finally we compared the different

107 chemical and compositions of PM<sub>2.5</sub> during two heaviest pollution episodes.

## 108 **2. Experimental section**

### 109 **2.1 Sample collection**

110 PM<sub>2.5</sub> samples were collected by using a high-volume sampler (Brand, USA) from 8<sup>th</sup>  
111 October to 24<sup>th</sup> November 2014 on the rooftop of a three-storey building located on the campus  
112 of China Research Academy of Environmental Sciences, which is situated in the north part of  
113 Beijing and close to the 5<sup>th</sup>-ring road. All the PM<sub>2.5</sub> samples were collected onto pre-baked (450  
114 °C for 8 h) quartz fiber filters (Whatman 41, USA). The duration of each sample collection is 23  
115 hr from 08:00 am of the previous day to 07:00 am of the next day. Field blanks were also  
116 collected before and after the campaign by mounting a pre-baked filter onto the sampler for 15  
117 min without pumping air. After collection, all the filter samplers were individually sealed in  
118 aluminum foil bags and stored in a freezer (-18 °C) prior to analysis. Daily values of SO<sub>2</sub>, NO<sub>x</sub>  
119 and meteorological parameters were cited from the website of Beijing Environmental Protection  
120 Agency.

### 121 **2.2 Sample analysis**

#### 122 **2.2.1 Elemental carbon (EC), organic carbon (OC), water-soluble organic (WSOC),** 123 **inorganic ions, aerosol liquid water content (ALWC) and aerosol acidity.**

124 Detailed methods for the analysis of EC, OC, WSOC and inorganic ions in aerosols were  
125 reported elsewhere (Li et al., 2011; Wang et al 2010). Briefly, EC and OC in the PM<sub>2.5</sub> samples  
126 were determined by using DRI Model 2001 Carbon analyzer following the Interagency  
127 Monitoring of Protected Visual Environments (IMPROVE) thermal/optical reflectance (TOR)  
128 protocol (Chow et al., 2007). WSOC and inorganic ions in the samples were extracted with

129 Milli-Q pure water and measured by using Shimadzu TOC-L CPH analyzer and Dionex-600 ion  
130 chromatography, respectively (Li et al. 2011; Wang et al 2010). In the current work, aerosol  
131 liquid water content (ALWC) and acidity (i.e., liquid  $H^+$  concentrations,  $[H^+]$ ) of the samples  
132 were calculated by using ISORROPIA-II model, which treated the  
133  $Na^+-NH_4^+-K^+-Ca^{2+}-Mg^{2+}-Cl^- -NO_3^- -SO_4^{2-}$  system and was performed in a “metastable” mode  
134 (Hennigan et al, 2015; Weber et al., 2016).

### 135 **2.2.2 Dicarboxylic acids, keto-carboxylic acids and $\alpha$ -dicarbonyls**

136 The method of analyzing  $PM_{2.5}$  samples for dicarboxylic acids, ketocarboxylic acids and  
137  $\alpha$ -dicarbonyl has been reported elsewhere (Wang et al., 2002, 2012; Meng et al., 2014; Cheng et  
138 al., 2015). Briefly, one eighth of the filter was extracted with Milli-Q water, concentrated to near  
139 dryness, and reacted with 14%  $BF_3$ /butanol at 100 °C for 1 h to convert aldehyde group into  
140 dibutoxy acetal and carboxyl group into butyl ester. Target compounds in the derivatized samples  
141 were identified by GC/MS and quantified by GC-FID (Agilent GC7890A).

### 142 **2.3. Stable carbon isotope composition of oxalic acid ( $C_2$ )**

143 Stable carbon isotope composition ( $\delta^{13}C$ ) of  $C_2$  was measured using the method developed  
144 by Kawamura and Watanabe (2004). Briefly,  $\delta^{13}C$  values of the derivatized samples above were  
145 determined by gas chromatography-isotope ratio-mass spectrometry (GC-IR-MS) (Thermo  
146 Fisher, Delta V Advantage). The  $\delta^{13}C$  value of  $C_2$  was then calculated from an isotopic mass  
147 balance equation based on the measured  $\delta^{13}C$  of the derivatizations and the derivatizing reagent  
148 (1-butanol) (Kawamura and Watanabe, 2004). Each sample was measured for three times to  
149 ensure the difference of the  $\delta^{13}C$  values less than 0.2‰, and the isotope data reported here is the  
150 averaged value of the triplicate measurements.

151 **3. Results and discussion**

152 **3.1 Variations in meteorological conditions, gaseous pollutants and major components of**  
153 **PM<sub>2.5</sub> during the Beijing 2014 APEC campaign**

154 Based on the emission control implementation for the APEC, we divided the whole study  
155 period into three phases: before-APEC (08/10 to 02/11), during-APEC (03/11 to 12/11) and  
156 after-APEC (13/11 to 24/11). Temporal variations in meteorological parameters and  
157 concentrations of gaseous pollutants and major components of PM<sub>2.5</sub> during the three phases are  
158 shown in Fig. 1 and summarized in Table 1.

159 Temperature during the sampling campaign showed a continuous decreasing trend with  
160 averages of  $13 \pm 2.6$  °C,  $7.0 \pm 1.7$  °C and  $4.3 \pm 1.3$  °C before-, during- and after-APEC periods,  
161 respectively, while relative humidity (RH) did not show a clear trend with mean values of  $62 \pm$   
162  $19\%$ ,  $47 \pm 14\%$  and  $51 \pm 16\%$  during the three periods (Fig.1a and Table 1). SO<sub>2</sub> showed a  
163 similar level before- and during-APEC periods ( $8.8 \pm 4.6$  μg m<sup>-3</sup> versus  $7.6 \pm 3.9$  μg m<sup>-3</sup>) (Table  
164 1), but increased dramatically to  $23 \pm 8.8$  μg m<sup>-3</sup> after-APEC due to domestic coal burning for  
165 house heating (Fig. 1b). NO<sub>2</sub> concentration ( $45 \pm 18$  μg m<sup>-3</sup>) during the APEC reduced by about  
166 30% compared to that in the before- and after-APEC phases ( $71 \pm 27$  μg m<sup>-3</sup> versus  $78 \pm 29$  μg  
167 m<sup>-3</sup>) (Table 1), mainly because of the reduction of the on-road vehicle numbers, as well as the  
168 reduced productivities of power plant and industry. O<sub>3</sub> displayed a decreasing trend similar to  
169 that of temperature (Fig. 1c). PM<sub>2.5</sub> pollution episodes in Beijing showed a periodic cycle of 4–5  
170 days, which is caused by the local weather cycles. Secondary inorganic ions (SIA, i.e., SO<sub>4</sub><sup>2-</sup>,  
171 NO<sub>3</sub><sup>-</sup> and NH<sub>4</sub><sup>+</sup>) are major components of PM<sub>2.5</sub> and present a temporal variation pattern similar  
172 to that of the fine particles (Fig. 1d). In the current work mass ratio of NO<sub>3</sub><sup>-</sup>/SO<sub>4</sub><sup>2-</sup> in PM<sub>2.5</sub>

173 during the whole study time is  $1.8 \pm 1.9$  (Table 1), which is in agreement with the ratio (1.6–2.4)  
174 for  $PM_1$  observed during the same time by using aerosol mass spectrometry (AMS) (Sun et al.,  
175 2016). OC and EC of  $PM_{2.5}$  linearly correlated each other ( $R^2=0.91$ ) and varied periodically in a  
176 cycle similar to SIA (Fig. 1e). OC/EC ratio during the whole sampling period is  $3.3 \pm 0.6$  (range:  
177 2.2–4.7) with no significant differences among the three APEC phases (Table 1).

178 Figure 2 shows the differences in chemical composition of  $PM_{2.5}$  before-, during- and  
179 after-APEC periods.  $PM_{2.5}$  is  $98 \pm 46 \mu g m^{-3}$  during-APEC, about 50% lower than that before-  
180 and after-APEC ( $178 \pm 122 \mu g m^{-3}$  versus  $161 \pm 100 \mu g m^{-3}$ ), respectively. Organic matter (OM)  
181 is the most abundant component of the fine particles. Relative abundance of OM (OM, 1.6 times  
182 of OC) (Xing et al., 2013) to  $PM_{2.5}$  continuously increased from 24% before-APEC to 30% and  
183 39% during- and after-APEC, respectively, although the mass concentration ( $19 \pm 7.6 \mu g m^{-3}$ ) of  
184 OC during-APEC is the lowest compared to those before- and after-APEC ( $26 \pm 16 \mu g m^{-3}$   
185 versus  $39 \pm 23 \mu g m^{-3}$ ). Sulfate, nitrate and ammonium before-APEC are  $15 \pm 13$ ,  $28 \pm 26$  and  
186  $9.0 \pm 8.0 \mu g m^{-3}$  (Table 1) and account for 8%, 16% and 5% of  $PM_{2.5}$ , respectively (Fig. 2). Their  
187 concentrations decrease to  $5.3 \pm 2.8$ ,  $10 \pm 8.1$  and  $3.1 \pm 2.6 \mu g m^{-3}$  (Table 1) with the relative  
188 contributions to  $PM_{2.5}$  down to 5%, 10% and 3% during-APEC, respectively. While after-APEC  
189 their concentrations increased to  $11 \pm 10$ ,  $15 \pm 13$  and  $6.9 \pm 6.4 \mu g m^{-3}$  and accounted for 7%,  
190 9% and 4% of  $PM_{2.5}$ . Such significant decreases in concentrations of OM and SIA during-APEC  
191 demonstrate the efficiency of the emission controls. OC/EC ratio is almost constant during the  
192 whole period, but WSOC/OC ratio decreased by 20% from  $0.42 \pm 0.13$  before-APEC,  $0.38 \pm$   
193  $0.16$  during-APEC to  $0.35 \pm 0.17$  after-APEC (Table 1). Since WSOC in fine aerosols consist  
194 mainly of secondary organic aerosols (SOA) (Laskin et al., 2015), the decreasing ratio of

195 WSOC/OC probably indicates a reduced SOA production during the campaign.

### 196 3.2 Oxalic acid and related SOA during the Beijing 2014 APEC campaign

197 A homogeneous series of dicarboxylic acids ( $C_2$ – $C_{11}$ ), keto-carboxylic acid and  
198  $\alpha$ -dicarbonyls in the  $PM_{2.5}$  samples were detected. As show in Table 2, total dicarboxylic acids  
199 during the whole study period is  $593 \pm 739 \text{ ng m}^{-3}$ , which is lower than that observed during  
200 Campaign of Air Quality Research in Beijing 2006 (CAREBeijing ) (average  $760 \text{ ng m}^{-3}$ ) and  
201 2007 (average  $1010 \text{ ng m}^{-3}$ ) (Ho et al, 2010, 2015) and the averaged wintertime concentration  
202 reported by a previous research for 14 Chinese cities ( $904 \text{ ng m}^{-3}$ ) (Ho et al, 2007). Total  
203 keto-carboxylic acid is  $66 \pm 81 \text{ ng m}^{-3}$ , while total dicarbonyls is  $126 \pm 115 \text{ ng m}^{-3}$  (Table 2).  
204 These values are higher than those during CAREBeijing 2006 and 2007 (Ho et al, 2010, 2015),  
205 but close to the value observed for the 14 Chinese megacities (Ho et al, 2007). Being similar to  
206 those previous observations, oxalic acid ( $C_2$ ) is the most abundant diacid in the 2014 APEC  
207 samples with an average of  $334 \pm 461 \text{ ng m}^{-3}$  (range: 10–2127  $\text{ng m}^{-3}$ , Table 2) during the whole  
208 campaign, followed by methylglyoxal (mGly), succinin acid ( $C_4$ ), terephthalic acid (tPh), and  
209 glyoxal (Gly). These five species account for 43%, 10%, 9%, 6% and 6% of total detected  
210 organic compounds (TDOC), respectively (Fig. 3).

211 As see in Fig. 4, TDOC in  $PM_{2.5}$  are  $1099 \pm 1104$ ,  $325 \pm 220$  and  $487 \pm 387 \text{ ng m}^{-3}$  before-,  
212 during- and after-APEC, respectively. In comparison with those before-APEC, TDOC  
213 during-APEC decreased by 71%. Oxalic acid ( $C_2$ ) is the leading species among the detected  
214 organic compounds and accounted for 46%, 31% and 34% of TDOC during the three phases,  
215 respectively (Fig. 4).  $C_2$  is an end product of precursors that are photochemically oxidized in  
216 aerosol aqueous phase via either oxidation of small compounds containing two carbon atoms or

217 decomposition of larger compounds containing three or more carbon atoms. Thus mass ratio of  
218 C<sub>2</sub> to TDOC is indicative of aerosol aging (Wang et al., 2012; Ho et al., 2015). As shown in Fig.  
219 4, the highest proportion of C<sub>2</sub> before- APEC suggests that organic aerosols during this period are  
220 more oxidized, compared to those during- and after-APEC. Glyoxal (Gly) and methylglyoxal  
221 (mGly) are the precursors of C<sub>2</sub>. Mass ratios of both compounds to TDOC are lowest  
222 before-APEC (Fig. 4). further indicating an enhanced SOA production during this period.

### 223 3.3 Formation mechanism of oxalic acid

#### 224 3.3.1 Correlation of oxalic acid with temperature, relative humidity (RH), aerosol liquid 225 water content (ALWC) and acidity and sulfate

226 A few studies have pointed out that aerosol aqueous phase oxidation is a major formation  
227 pathway for oxalic acid (Yu et al., 2005; Pinxteren, et al., 2014; Bikkina et al., 2015; Tilgner et al.,  
228 2010). To explore the formation mechanism of oxalic acid, we calculated ALWC and acidity (i.e.,  
229 proton concentration, [H<sup>+</sup>]) of PM<sub>2.5</sub> aerosols by using ISOROPPIA-II model (Weber et al.,  
230 2016). As shown in Fig. 5, during the entire period C<sub>2</sub> showed a strong linear correlation with  
231 sulfate (R<sup>2</sup>=0.70 Fig. 5a), which is consistent with those observed in Xi'an (Wang et al., 2012)  
232 and other Chinese cities (Yu et al., 2005). Previous studies on particle morphology showed that  
233 sulfate particles internally mixes with SOA in Beijing especially in humid haze days (Li et al.,  
234 2010, 2011), which probably indicates that they are formed via similar aqueous phase pathways.  
235 In addition, a robust correlation was also found for C<sub>2</sub> with RH (R<sup>2</sup>=0.64, Fig. 5b) and aerosol  
236 liquid water content (ALWC) (R<sup>2</sup>=0.61, Fig. 5c), indicating that humid conditions are favorable  
237 for the aqueous phase formation of C<sub>2</sub>, which is most likely due to an enhanced gas-to-aerosol



238 aqueous phase partitioning of the precursors (e.g., Gly and mGly) (Fu et al., 2008; Wang et al.,  
239 2015).

240  $\text{NH}_4^+$ ,  $\text{NO}_3^-$  and  $\text{SO}_4^{2-}$  are the dominant cation and anions of fine particles in Beijing,  
241 respectively (Guo et al., 2014; Zhang et al., 2015) and the molar ratio of  $[\text{NH}_4^+]$  to  $[\text{NO}_3^- + \text{SO}_4^{2-}]$   
242 in this study is 1.1. Thus it is plausible that  $\text{SO}_4^{2-}$  during the APEC campaign largely existed as  
243 ammonium bisulfate, resulting in a strong linear correlation between  $[\text{H}^+]$  and  $\text{SO}_4^{2-}$  with a molar  
244 slope of 1.03 (Fig. 5d) (Zhang et al., 2007). In addition,  $[\text{H}^+]$  shows a significant positive  
245 correlation with  $\text{C}_2$  ( $R^2 = 0.84$ ) (Fig. 5e), possibly due to the fact that acidic conditions are  
246 favorable for the formation of  $\text{C}_2$  precursors. For example, Surratt et al (2007; 2010) found that  
247 aerosol acidity can promote the formation of biogenic SOA (BSOA) derived from isoprene  
248 oxidation such as 2-methylglyceric acid, Gly and mGly. These BSOA precursors can be further  
249 oxidized into  $\text{C}_2$  (Meng et al., 2014; Wang et al., 2009).

250 There is a significant positive correlation ( $R^2 = 0.58$ ,  $p < 0.001$ ) between the mass ratios of  
251  $\text{C}_2/\text{TDOC}$  and ambient temperatures (Fig. 5f), which is similar to the results found by previous  
252 researchers (Ho et al., 2007; Strader et al., 1999), indicating that organic aerosols are more aged  
253 under a higher temperature condition (Erven et al, 2011; Carlton et al., 2009). Thus, compared  
254 with those before-APEC the lower  $\text{C}_2/\text{TDOC}$  ratios (31% and 34%, respectively) (Fig. 4) during-  
255 and after-APEC can be ascribed in part to the relatively lower temperature conditions that are not  
256 favorable for oxidation of the precursors to produce oxalic acid ( $13 \pm 2.6$  °C,  $7.0 \pm 1.7$  °C and  
257  $4.3 \pm 1.3$  °C before-, during- and after-APEC periods, respectively) (Table 1).

### 258 3.3.2 Temporal variation in stable carbon isotopic composition of oxalic acid

259 To further discuss the formation mechanism of  $\text{C}_2$ , we investigated the temporal variations

260 of concentration and stable carbon isotopic composition of C<sub>2</sub> in the PM<sub>2.5</sub> samples (Fig. 6).  
261 Previous studies have demonstrated that Gly, mGly, glyoxylic acid ( $\omega$ C<sub>2</sub>) and pyruvic acid (Pyr)  
262 are the precursors of C<sub>2</sub> (Carlton et al., 2006, 2007; Ervens and Barbara, 2004; Wang et al., 2012).  
263 Thus, higher mass ratios of C<sub>2</sub> to its precursors indicate that organic aerosols are more oxidized  
264 (Wang et al., 2010). As shown in Table 3,  $\delta^{13}\text{C}$  of C<sub>2</sub> in this work positively correlated with the  
265 mass ratios of C<sub>2</sub>/ $\omega$ C<sub>2</sub>, C<sub>2</sub>/mGly and TDOC/WSOC, demonstrating an enrichment of <sup>13</sup>C during  
266 the aerosol oxidation process. Because decomposition (or breakdown) of larger molecular weight  
267 precursors in aerosol aqueous phase is the dominant formation pathway for C<sub>2</sub> in aerosol ageing  
268 process (Kawamura et al., 2016; Gensch et al., 2014; Kirillova et al., 2013), during which  
269 organic compounds release CO<sub>2</sub>/CO by reaction with OH radical and other oxidants, resulting in  
270 the evolved species enriched with lighter isotope (<sup>12</sup>C) and the remaining substrate enriched in  
271 <sup>13</sup>C due to kinetic isotope effects (KIE) (Hoefs, 1997; Rudolph et al., 2002).

272 72-h backward trajectory analysis showed that air masses moved to Beijing during the  
273 whole sampling period can roughly be categorized into three types (Fig. 6a) (all trajectories  
274 during the entire study period can be found in the supplementary materials). (1) **Polluted type**, by  
275 which air masses originated from inland and east coastal China and moved slowly into Beijing  
276 within 72-h from its south regions, i.e., Henan, Shandong and Jiangsu Provinces. **This type of air**  
277 **masses mostly occurred before-APEC with high PM<sub>2.5</sub> concentrations.** Air pollution has widely  
278 distributed in the three provinces (Wei et al., 2016); thus aerosols transported by this type of air  
279 masses are of regional characteristics. (2) **Mixed type**, by which air masses originated from  
280 Mongolia and North China, and moved quickly into Hebei province and then turned back to  
281 Beijing. Air in Mongolia and North China was clean but polluted in Hebei province, which is

282 adjacent to Beijing. This type of air masses is a mixture of clean and polluted air and thus named  
283 as mixed type. Since the resident time of the mixed type of air masses within Hebei province is  
284 very short, thus aerosols transported by this type of air masses is of local characteristics and  
285 relatively fresh. (3) Clean type, by which air masses originated from Siberia and moved rapidly  
286 into Beijing directly via a long-range transport. Aerosols from the clean type of air masses are  
287 much more aged, while those from the mixed type of air masses are fresh. Since severe air  
288 pollution is widespread in the south regions, gas-to-aerosol phase partitioning of precursors and  
289 subsequent aerosol-phase oxidation to produce SOA including C<sub>2</sub> continuously proceed during  
290 the air mass movement. However, such a partition for producing SOA is not significant when air  
291 mass move from Siberia, Mongolia and North China because of the much less abundant VOCs.  
292 In stead, aerosols in the clean air masses are continuously oxidized, during which C<sub>2</sub> is produced  
293 by photochemical decomposition of larger molecular weight precursors. Therefore, C<sub>2</sub> in PM<sub>2.5</sub>  
294 transported by the mixed type air masses are not only fresh and abundant but also enriched in <sup>12</sup>C,  
295 whereas C<sub>2</sub> in PM<sub>2.5</sub> transported by the clean type air masses are aged, less abundant and  
296 enriched in <sup>13</sup>C due to KIE effects, as illustrated by the pink and light blue columns in Fig. 6b,  
297 respectively. C<sub>2</sub> in PM<sub>2.5</sub> transported by the polluted type of air masses are most abundant  
298 compared with that in other two type of air masses, which is not only due to the severe air  
299 pollution in the Henan, Shandong and Jiangsu provinces but also due to the enhanced  
300 photochemical oxidation under the humid, higher temperature and stagnant conditions that  
301 occurred mostly before-APEC, as discussed previously. Therefore, C<sub>2</sub> in the polluted type of air  
302 masses is not only abundant but also enriched in <sup>13</sup>C (see black columns in Fig. 6b).

### 303 3.4 Different chemical characteristics of PM<sub>2.5</sub> between two severe haze events

304 From Fig. 1 and Table 4, it can be found that PM<sub>2.5</sub> showed two equivalent maxima on 9<sup>th</sup>  
305 October and 20<sup>th</sup> November during the whole study period. However, the chemical compositions  
306 of PM<sub>2.5</sub> during these two pollution events were significantly different. As shown in Fig. 7a,  
307 relative abundances of SIA (sum of SO<sub>4</sub><sup>2-</sup>, NO<sub>3</sub><sup>-</sup> and NH<sub>4</sub><sup>+</sup>) to PM<sub>2.5</sub> are 30% during the event I  
308 and 23% during the event II, respectively. The relative abundance of OM (21%, Fig. 7a) during  
309 the event I is lower than that (37%) during the event II (Fig. 7b). In contrast, the ratios of  
310 WSOC/OC and TDOC/OC are higher in the event I than in the event II, which is consistent with  
311 lower levels of O<sub>3</sub> after-APEC (Table 1), suggesting a weaker photochemical oxidation capacity  
312 during the event II. Organic biomarkers in the PM<sub>2.5</sub> have been measured for the source  
313 apportionment (Wang et al., 2016) and cited here to further identify the difference in chemical  
314 composition of PM<sub>2.5</sub> between the two events. Levoglucosan is a key tracer for biomass burning  
315 smoke. Mass ratio of levoglucosan to OC in PM<sub>2.5</sub> (Lev/OC) is comparable between the two  
316 events, suggesting a similar level of contributions of biomass burning emission to PM<sub>2.5</sub> before-  
317 and after-APEC. However, the mass ratios of PAHs and hopanes to OC are lower in event I than  
318 those in event II (Fig. 7c), which again demonstrates the enhanced emissions from coal burning  
319 for house heating, because these compounds are key tracers of coal burning smokes (Wang et al.,  
320 2006). As seen in Fig. 7d, C<sub>2</sub> in the event I was enriched in <sup>13</sup>C. Such relatively more abundant  
321 SIA, WSOC and TDOC and heavier C<sub>2</sub> in PM<sub>2.5</sub> clearly demonstrate that PM<sub>2.5</sub> during the event  
322 I were enriched with secondary products while the fine particles during the event II were  
323 enriched with primary compounds. After-APEC house heating activities including residential  
324 coal burning were activated, which emitted huge amounts of SO<sub>2</sub>, NO<sub>x</sub>, and VOCs as well as  
325 primary particles, resulting in both absolute concentrations and relative abundances of CO and

326 EC 30–40% higher after-APEC than before-APEC (see Table 1). Li et al (2015) reported that  
327 VOCs in Beijing was 86 ppbv before-APEC, 48 ppbv during-APEC and 73 ppbv after-APEC. As  
328 shown in Table 4, temperature ( $16.7\pm 0.8$  °C for event I and  $4.5\pm 1.7$  °C for event II) and relative  
329 humidity (RH) ( $82\pm 4\%$  for event I and  $62\pm 13\%$  for event II) are lower during the event II than  
330 during the event I. Moreover, air masses arriving in Beijing during the event II are the mix type,  
331 of which the resident time in Hebei province is short. Compared with those in the event I, such  
332 colder and drier conditions and short reaction time during the event II are unfavorable for  
333 photochemical oxidation, resulting in SOA not only less abundant but also enriched with lighter  
334  $^{12}\text{C}$  during the event II, although VOCs levels are comparable before- and after-APEC.

#### 335 4. Summary and conclusion

336 Temporal variations in molecular distribution of SIA, dicarboxylic acids, ketoacids and  
337  $\alpha$ -dicarbonyl and stable carbon isotopic composition ( $\delta^{13}\text{C}$ ) of  $\text{C}_2$  in  $\text{PM}_{2.5}$  collected in Beijing  
338 before-, during- and after- the 2014 APEC were investigated. Absolute concentrations and  
339 relative abundances of SIA and  $\text{C}_2$  in  $\text{PM}_{2.5}$  are highest before-APEC, followed by those after-  
340 and during-APEC, suggesting that the fine aerosols before-APEC are enriched with secondary  
341 products, mainly due to an enhanced photochemical oxidation under the warm, humid and  
342 stagnant conditions. Concentrations of SIA, oxalic acid and related SOA in  $\text{PM}_{2.5}$  during-APEC  
343 are 2–4 times lower than those before-APEC, which can be ascribed to the effective emission  
344 controls and the favorable meteorological conditions that brought clean air from Siberia and  
345 Mongolia into Beijing.

346 Positive correlations of  $\text{C}_2$  with RH, sulfate mass, ALWC and aerosol acidity indicate that  
347  $\text{C}_2$  formation pathway is involved an acid-catalyzed aerosol aqueous phase oxidation. SIA,  $\text{C}_2$

348 and related SOA in the polluted type of air masses are abundant with C<sub>2</sub> enriched in <sup>13</sup>C. On the  
349 contrary, those in the clean type of air masses are much less abundant, although C<sub>2</sub> is also  
350 enriched in <sup>13</sup>C. By comparing the chemical composition of PM<sub>2.5</sub> and δ<sup>13</sup>C values of C<sub>2</sub> in two  
351 events that are characterized by the highest loadings of PM<sub>2.5</sub> before- and after-APEC, we further  
352 found that compared with those before- APEC fine aerosols after-APEC are enriched with  
353 primary species and C<sub>2</sub> is depleted in heavier <sup>13</sup>C, although SO<sub>2</sub>, NO<sub>x</sub> and VOCs are abundant  
354 during the heating season, again demonstrating the important role of meteorological conditions  
355 in the secondary aerosol formation process, which are warmer, humid and stagnant before-APEC  
356 and result in secondary species much more abundant than those during- and after-APEC.

357

### 358 **Acknowledgements**

359 This work was financially supported by the Strategic Priority Research Program of the  
360 Chinese Academy of Sciences (Grants No. XDB05020401), the China National Natural Science  
361 Funds for Distinguished Young Scholars (Grants No. 41325014), and the program from  
362 National Nature Science Foundation of China (No. 41405122, 91544226 and 41375132 ).

363

364

### 365 **References**

- 366 Bikkina, S., Kawamura, K., and Miyazaki, Y.: Latitudinal distributions of atmospheric dicarboxylic acids,  
367 oxocarboxylic acids, and α-dicarbonyls over the western North Pacific: Sources and formation pathways, *Journal*  
368 *of Geophysical Research: Atmospheres*, 120, 5010-5035, 10.1002/2014jd022235, 2015.
- 369 Carlton, A. G., Turpin, B. J., Lim, H.-J., Altieri, K. E., and Seitzinger, S.: Link between isoprene and secondary  
370 organic aerosol (SOA): Pyruvic acid oxidation yields low volatility organic acids in clouds, *Geophysical*  
371 *Research Letters*, 33, 10.1029/2005gl025374, 2006.
- 372 Carlton, A. G., Turpin, B. J., Altieri, K. E., Seitzinger, S., Reff, A., Lim, H.-J., and Ervens, B.: Atmospheric oxalic  
373 acid and SOA production from glyoxal: Results of aqueous photooxidation experiments, *Atmos. Environ.*, 41,  
374 7588-7602, 2007.
- 375 Carlton, A., Wiedinmyer, C., and Kroll, J.: A review of Secondary Organic Aerosol (SOA) formation from isoprene,  
376 *Atmos. Chem. Phys.*, 9, 4987-5005, 2009.
- 377 Cheng, C., Wang, G., Meng, J., Wang, Q., Cao, J., Li, J., and Wang, J.: Size-resolved airborne particulate oxalic and  
378 related secondary organic aerosol species in the urban atmosphere of Chengdu, China, *Atmospheric Research*,  
379 161-162, 134-142, 10.1016/j.atmosres.2015.04.010, 2015.

380 Chow, J. C., Watson, J. G., Chen, L.-W. A., Chang, M. O., Robinson, N. F., Trimble, D., and Kohl, S.: The  
381 IMPROVE\_A temperature protocol for thermal/optical carbon analysis: maintaining consistency with a  
382 long-term database, *Journal of the Air & Waste Management Association*, 57, 1014-1023, 2007.

383 Ervens, B.: A modeling study of aqueous production of dicarboxylic acids: 1. Chemical pathways and speciated  
384 organic mass production, *J. Geophys. Res.*, 109, 10.1029/2003jd004387, 2004.

385 Ervens, B., Turpin, B. J., and Weber, R. J.: Secondary organic aerosol formation in cloud droplets and aqueous  
386 particles (aqSOA): a review of laboratory, field and model studies, *Atmos. Chem. Phys.*, 11, 11069-11102, 2011.

387 Fu, T.-M., Jacob, D. J., Wittrock, F., Burrows, J. P., Vrekoussis, M., and Henze, D. K.: Global budgets of  
388 atmospheric glyoxal and methylglyoxal, and implications for formation of secondary organic aerosols, *J.*  
389 *Geophys. Res.*, 113, D15303, doi:10.1029/2007JD009505, 2008.

390 Gao, S., Ng, N. L., Keywood, M., Varutbangkul, V., Bahreini, R., Nenes, A., He, J., Yoo, K. Y., Beauchamp, J. L.,  
391 Hodyss, R. P., Flagan, R. C., and Seinfeld, J. H.: Particle phase acidity and oligomer formation in secondary  
392 organic aerosol, *Environ. Sci. Technol.*, 38, 6582-6589, 2004.

393 Gensch, I., Kiendler-Scharr, A., and Rudolph, J.: Isotope ratio studies of atmospheric organic compounds: Principles,  
394 methods, applications and potential, *International Journal of Mass Spectrometry*, 365-366, 206-221,  
395 10.1016/j.ijms.2014.02.004, 2014.

396 Guo, S., Hu, M., Zamora, M. L., Peng, J., Shang, D., Zheng, J., Du, Z., Wu, Z., Shao, M., Zeng, L., Molina, M. J.,  
397 and Zhang, R.: Elucidating severe urban haze formation in China, *Proceedings of the National Academy of*  
398 *Sciences*, 111(49), 17373-17378, 2014.

399 Hennigan, C. J., Izumi, J., Sullivan, A. P., Weber, R. J., and Nenes, A.: A critical evaluation of proxy methods used  
400 to estimate the acidity of atmospheric particles, *Atmos. Chem. Phys.*, 15(5), 2775-2790, 2015.

401 Ho, K. F., Cao, J. J., Lee, S. C., Kawamura, K., Zhang, R. J., Chow, J. C., and Watson, J. G.: Dicarboxylic acids,  
402 ketocarboxylic acids, and dicarbonyls in the urban atmosphere of China, *J. Geophys. Res.*, 112,  
403 10.1029/2006jd008011, 2007.

404 Ho, K. F., Lee, S. C., Ho, S. S. H., Kawamura, K., Tachibana, E., Cheng, Y., and Zhu, T.: Dicarboxylic acids,  
405 ketocarboxylic acids,  $\alpha$ -dicarbonyls, fatty acids, and benzoic acid in urban aerosols collected during the 2006  
406 Campaign of Air Quality Research in Beijing (CAREBeijing-2006), *J. Geophys. Res.*, 115,  
407 10.1029/2009jd013304, 2010.

408 Ho, K. F., Huang, R. J., Kawamura, K., Tachibana, E., Lee, S. C., Ho, S. S. H., Zhu, T., and Tian, L.: Dicarboxylic  
409 acids, ketocarboxylic acids,  $\alpha$ -dicarbonyls, fatty acids and benzoic acid in PM<sub>2.5</sub> aerosol collected during  
410 CAREBeijing-2007: an effect of traffic restriction on air quality, *Atmospheric Chemistry and Physics*, 15,  
411 3111-3123, 10.5194/acp-15-3111-2015, 2015.

412 Hoefs, J., *Stable Isotope Geochemistry.*, Springer, New York, 1997.

413 Huang, R. J., Zhang, Y., Bozzetti, C., Ho, K. F., Cao, J. J., Han, Y., Daellenbach, K. R., Slowik, J. G., Platt, S. M.,  
414 Canonaco, F., Zotter, P., Wolf, R., Pieber, S. M., Brun, E. A., Crippa, M., Ciarelli, G., Piazzalunga, A.,  
415 Schwikowski, M., Abbaszade, G., Schnelle-Kreis, J., Zimmermann, R., An, Z., Szidat, S., Baltensperger, U., El  
416 Haddad, I., and Prevot, A. S.: High secondary aerosol contribution to particulate pollution during haze events in  
417 China, *Nature*, 514, 218-222, 10.1038/nature13774, 2014.

418 Kawamura, K., and Bikkina, S.: A review of dicarboxylic acids and related compounds in atmospheric aerosols:  
419 Molecular distributions, sources and transformation, *Atmospheric Research*, 170, 140-160, 2016.

420 Kawamura, K., and Watanabe, T.: Determination of stable carbon isotopic compositions of low molecular weight  
421 dicarboxylic acids and ketocarboxylic acids in atmospheric aerosol and snow samples, *Analytical Chemistry*, 76,  
422 5762-5768, 2004.

423 Kawamura, K., and Bikkina, S.: A review of dicarboxylic acids and related compounds in atmospheric aerosols:  
424 Molecular distributions, sources and transformation, *Atmospheric Research*, 10.1016/j.atmosres.2015.11.018,  
425 2015.

426 Kirillova, E. N., Andersson, A., Sheesley, R. J., Kruså, M., Praveen, P. S., Budhavant, K., Safai, P. D., Rao, P. S. P.,  
427 and Gustafsson, Ö.: <sup>13</sup>C- and <sup>14</sup>C-based study of sources and atmospheric processing of water-soluble organic  
428 carbon (WSOC) in South Asian aerosols, *J. Geophys. Res.*, 118, 614-626, 2013.

429 Li, J., Xie, S. D., Zeng, L. M., Li, L. Y., Li, Y. Q., and Wu, R. R.: Characterization of ambient volatile organic  
430 compounds and their sources in Beijing, before, during, and after Asia-Pacific Economic Cooperation China  
431 2014, *Atmos. Chem. Phys.*, 15, 7945-7959, 2015.

432 Li, W.J. and Shao, L.Y.: Mixing and water-soluble characteristics of particulate organic compounds in individual  
433 urban aerosol particles. *J. Geophys. Res.* 115 (D02301), doi:10.1029/2009JD012575, 2010.

434 Li, W.J., Zhou, S.Z., Wang, X.F., Xu, Z., Yuan, C., Yu, Y.C., Zhang, Q.Z. and Wang, W.X.: Integrated evaluation  
435 of aerosols from regional brown hazes over northern China in winter: Concentrations, sources, transformation,  
436 and mixing states. *J. Geophys. Res.* 116 (D9), doi:10.1029/2010JD015099,2011.

437 Laskin, A., Laskin, J., and Nizkorodov, S. A.: Chemistry of atmospheric brown carbon, *Chem. Rev.*, 115,  
438 4335-4382, 2015.

439 Meng, J., Wang, G., Li, J., Cheng, C., Ren, Y., Huang, Y., Cheng, Y., Cao, J., and Zhang, T.: Seasonal  
440 characteristics of oxalic acid and related SOA in the free troposphere of Mt. Hua, central China: implications for  
441 sources and formation mechanisms, *Sci Total Environ*, 493, 1088-1097, 2014.

442 Mu Quan, Z. S.: An evaluation of the economic loss due to the heavy haze during January 2013 in China., *China  
443 Environmental Science*, 33, 2087-2094, 2013.

444 Pathak, R. K., Wang, T., Ho, K. F., and Lee, S. C.: Characteristics of summertime PM<sub>2.5</sub> organic and elemental  
445 carbon in four major Chinese cities: Implications of high acidity for water-soluble organic carbon (WSOC),  
446 *Atmos. Environ.*, 45, 318-325, 10.1016/j.atmosenv.2010.10.021, 2011.

447 Rudolph, J., Czuba, E., Norman, A., Huang, L., and Ernst, D.: Stable carbon isotope composition of nonmethane  
448 hydrocarbons in emissions from transportation related sources and atmospheric observations in an urban  
449 atmosphere, *Atmos. Environ.*, 36, 1173-1181, 2002.

450 Strader, R., Lurmann, F., and Pandis, S. N.: Evaluation of secondary organic aerosol formation in winter, *Atmos.  
451 Environ.*, 33, 4849-4863, 1999.

452 Sullivan, R. C., and Prather, K. A.: Investigations of the diurnal cycle and mixing state of oxalic acid in individual  
453 particles in Asian aerosol outflow, *Environ. Sci. Technol.*, 41, 8062-8069, 2007.

454 Sun, Y., Wang, Z., Wild, O., Xu, W., Chen, C., Fu, P., Du, W., Zhou, L., Zhang, Q., Han, T., Wang, Q., Pan, X.,  
455 Zheng, H., Li, J., Guo, X., Liu, J., and Worsnop, D. R.: "APEC Blue": Secondary Aerosol Reductions from  
456 Emission Controls in Beijing, *Scientific reports*, 6, 20668, 10.1038/srep20668, 2016.

457 Surratt, J. D., Lewandowski, M., Offenberg, J. H., Jaoui, M., Kleindienst, T. E., Edney, E. O., and Seinfeld, J. H.:  
458 Effect of Acidity on Secondary Organic Aerosol Formation from Isoprene, *Environ. Sci. Technol.*, 41,  
459 5363-5369, 2007.

460 Surratt, J. D., Chan, A. W. H., Eddingsaas, N. C., Chan, M., Loza, C. L., Kwan, A. J., Hersey, S. P., Flagan, R. C.,  
461 Wennberg, P. O., and Seinfeld, J. H.: Reactive intermediates revealed in secondary organic aerosol formation  
462 from isoprene, *Proceedings of National Academy of Science of United States of America*, 107, 6640-6645,  
463 2010.

464 Tang, G., Zhu, X., Hu, B., Xin, J., Wang, L., Münkel, C., Mao, G., and Wang, Y.: Impact of emission controls on  
465 air quality in Beijing during APEC 2014: lidar ceilometer observations, *Atmos. Chem. Phys.*, 15, 12667-12680,  
466 2015.



467 Tilgner, A. and Herrmann, H.: Radical-driven carbonyl-to-acid conversion and acid degradation in tropospheric  
468 aqueous systems studied by CAPRAM. *Atmos. Environ.*, 44, 5415-5422, 2010.

469 Van Donkelaar, A., Martin, R. V., Brauer, M., Kahn, R., Levy, R., Verduzco, C., and Villeneuve, P. J.: Global  
470 estimates of ambient fine particulate matter concentrations from satellite-based aerosol optical depth:  
471 development and application, University of British Columbia, 2015.

472 van Pinxteren, D., Neusüß, C., and Herrmann, H.: On the abundance and source contributions of dicarboxylic acids  
473 in size-resolved aerosol particles at continental sites in central Europe, *Atmos. Chem. Phys.*, 14, 3913-3928,  
474 2014.

475 Wang, G., Cheng, C., Meng, J., Huang, Y., Li, J. and Ren, Y.: Field observation on secondary organic aerosols  
476 during Asian dust storm periods: Formation mechanism of oxalic acid and related compounds on dust surface.  
477 *Atmos. Environ.*, 113, 169-176, 2015.

478 Wang, G. H., Kawamura, K., Lee, S. C., Ho, K. F. and Cao, J. J.: Molecular, seasonal and spatial distributions of  
479 organic aerosols from fourteen Chinese cities. *Environ. Sci. Technol.*, 40, 4619-4625, 2006.

480 Wang, G., Kawamura, K., Umemoto, N., Xie, M., Hu, S. and Wang, Z.: Water-soluble organic compounds in  
481 PM<sub>2.5</sub> and size-segregated aerosols over Mt. Tai in North China Plain. *Journal of Geophysical  
482 Research-Atmospheres*, 114, D19208, doi.10.1029/2008JD011390, 2009.

483 Wang, G., Kawamura, K., Cheng, C., Li, J., Cao, J., Zhang, R., Zhang, T., Liu, S., and Zhao, Z.: Molecular  
484 distribution and stable carbon isotopic composition of dicarboxylic acids, ketocarboxylic acids, and  
485 alpha-dicarbonyls in size-resolved atmospheric particles from Xi'an City, China, *Environ. Sci. Technol.*, 46,  
486 4783-4791, 2012.

487 Wang, G., Niu, S, Liu, C., and Wang, L.: Identification of dicarboxylic acids and aldehydes of PM<sub>10</sub> and PM<sub>2.5</sub>  
488 aerosols in Nanjing, China, *Atmospheric Environment*, 36(12), 1941-1950, 2002.

489 Wang, G., Xie, M., Hu, S., Gao, S., Tachibana, E., and Kawamura, K.: Dicarboxylic acids, metals and isotopic  
490 compositions of C and N in atmospheric aerosols from inland China: implications for dust and coal burning  
491 emission and secondary aerosol formation, *Atmos. Chem. Phys.*, 10, 6087-6096, 2010.

492 Wang, G., Wang, J., Ren, Y. and Li, J.: Chemical characterization of organic aerosols from Beijing during the 2014  
493 APEC (under preparation), 2016.

494 Wang, G., Zhang, R., Zamora, M. L., Gomez, M. E., Yang, L., Hu, M., Lin, Y., Guo, S., Meng, J., Li, J., Cheng, C.,  
495 Hu, T., Ren, Y., Wang, Y., Gao, J., Cao, J., An, Z., Zhou, W., Jiayuan Wang, Marrero-Ortiz, W., Tian, P.,  
496 Secret, J., Peng, J., Du, Z., Jing Zheng, Shang, D., Zeng, L., Shao, M., Wang, W., Huang, Y., Wang, Y., Zhu,  
497 Y., Li, Y., Hu, J., Pan, B., Cai, L., Cheng, Y., Rosenfeld, D., Liss, P. S., Duce, R. A., Kolb, C. E., and Molina, M.  
498 J.: Persistent Sulfate Formation from London Fog to Chinese Haze, *Proceedings of National Academy of  
499 Science of United States of America*, doi/10.1073/pnas.1616540113., 2016.

500 Wang, Y., Zhang, Q. Q., He, K., Zhang, Q., and Chai, L.: Sulfate-nitrate-ammonium aerosols over China: response  
501 to 2000–2015 emission changes of sulfur dioxide, nitrogen oxides, and ammonia, *Atmos. Chem. Phys.*, 13,  
502 2635-2652, 2013.

503 Weber, R. J., Guo, H., Russell, A. G., and Nenes, A.: High aerosol acidity despite declining atmospheric sulfate  
504 concentrations over the past 15 years, *Nature Geoscience*, 9, 282-285, 10.1038/ngeo2665, 2016.

505 Wei, X., Gu, X., Chen, H., Cheng, T., Wang, Y., Guo, H., Bao, F., and Xiang, K.: Multi-Scale Observations of  
506 Atmosphere Environment and Aerosol Properties over North China during APEC Meeting Periods, *Atmosphere*,  
507 7(1), 2016.

508 Xing, L., Fu, T. M., Cao, J. J., Lee, S. C., Wang, G. H., Ho, K. F., Cheng, M. C., You, C. F., and Wang, T. J.:  
509 Seasonal and spatial variability of the OM/OC mass ratios and high regional correlation between oxalic acid and  
510 zinc in Chinese urban organic aerosols, *Atmos. Chem. Phys.*, 13, 4307-4318, 2013.

511 Xu, W. Q., Sun, Y. L., Chen, C., Du, W., Han, T. T., Q. Wang, Q., Fu, P. Q., F. Wang, Z., Zhao, X. J., Zhou, L. B., Ji,  
512 D. S., Wang, P. C., and Worsnop, D. R.: Aerosol composition, oxidation properties, and sources in Beijing:  
513 results from the 2014 Asia-Pacific Economic Cooperation summit study, *Atmos. Chem. Phys.*, 15, 13681–13698,  
514 2015.

515 Yu, J. Z., Huang, X.-F., Xu, J., and Hu, M.: When Aerosol Sulfate Goes Up, So Does Oxalate: Implication for the  
516 Formation Mechanisms of Oxalate, *Environ. Sci. Technol.*, 39, 128-133, 2005.

517 Zhang, Q., Jimenez, J. L., Worsnop, D. R., and Canagaratna, M.: A case study of urban particle acidity and its  
518 influence on secondary organic aerosol, *Environ. Sci. Technol.*, 41, 3213-3219, 2007.

519 Zhang, Q., Streets, D. G., Carmichael, G. R., He, K., Huo, H., Kannari, A., Klimont, Z., Park, I., Reddy, S., and Fu,  
520 J.: Asian emissions in 2006 for the NASA INTEX-B mission, *Atmos. Chem. Phys.*, 9, 5131-5153, 2009.

521 Zhang, R., Wang, G., Guo, S., Zamora, M. L., Ying, Q., Lin, Y., Wang, W., Hu, M., and Wang, Y.: Formation of  
522 urban fine particulate matter, *Chemical Reviews*, 115, 3803-3855, 2015.

523 Zheng, G. J., Duan, F. K., Su, H., Ma, Y. L., Cheng, Y., Zheng, B., Zhang, Q., Huang, T., Kimoto, T., Chang, D.,  
524 Pöschl, U., Cheng, Y. F., and He, K. B.: Exploring the severe winter haze in Beijing: the impact of synoptic  
525 weather, regional transport and heterogeneous reactions, *Atmos. Chem. Phys.*, 15, 2969-2983, 2015.

526

527 **Figure Captions**

528

529 **Figure 1.** Temporal variations of meteorological conditions, gaseous pollutants and major  
530 components of PM<sub>2.5</sub> during the 2014 APEC campaign. (The brown shadows  
531 represent two air pollution events characterized by highest PM<sub>2.5</sub> levels before- and  
532 after-APEC, while the blue shadow represents the APEC event).

533

534 **Figure 2.** Chemical composition of PM<sub>2.5</sub> during the 2014 APEC campaign.

535

536 **Figure 3.** Molecular distributions of dicarboxylic acids and related compounds in PM<sub>2.5</sub> of  
537 Beijing, China during the 2014 APEC campaign. The pie chart is the average  
538 composition of total detected organic compounds (TDOC) and the top number is the  
539 average mass concentration of TDOC of the whole study period.

540

541 **Figure 4.** Compositions of total detected organic compounds (TDOC) in PM<sub>2.5</sub> during the 2014  
542 APEC campaign.

543

544 **Figure 5.** Correlation analysis for oxalic acid (C<sub>2</sub>) and sulfate in PM<sub>2.5</sub> during the whole 2014  
545 APEC campaign. **(a-c)** Concentrations of C<sub>2</sub> with sulfate, relative humidity (RH), and  
546 aerosol liquid water content (ALWC); **(d, e)** sulfate and C<sub>2</sub> with aerosol acidity [H<sup>+</sup>]  
547 and **(f)** temperature with mass ratio of C<sub>2</sub> to total detected organic compounds  
548 (C<sub>2</sub>/TDOC).

549

550 **Figure 6.** **(a)** 72-h backward trajectories determined by the National Oceanic and Atmospheric  
551 Administration Hybrid Single Particle Lagrangian Integrated Trajectory (HYSPLIT)  
552 model arriving at the sampling site to reveal the major air mass flow types during the  
553 study period. Northwesterly wind (light blue) was most frequently (64%), followed by  
554 northerly (21%, pink) and southerly (15%, black) and is defined as clean, mixed and  
555 polluted types, respectively (see the definitions in the text); **(b)** Time series of δ<sup>13</sup>C  
556 values and concentration of oxalic acid during the whole study period (Colors in Fig.  
557 6a are corresponding to those in Fig. 6b).

558

559 **Figure 7.** Comparison of chemical composition of PM<sub>2.5</sub> during two air pollution events. **(a)**  
560 Percentages of major species in PM<sub>2.5</sub>; **(b, c)** mass ratios of major species and organic  
561 tracers in PM<sub>2.5</sub>; **(d)** stable carbon isotope composition of oxalic acid (C<sub>2</sub>) (Data about  
562 levoglucosan (Lev), PAHs and hopanes are cited from Wang et al (2016)).

563

564  
565  
566  
567  
568  
569  
570  
571  
572  
573  
574  
575  
576  
577  
578  
579  
580  
581  
582  
583  
584  
585  
586  
587  
588  
589  
590

Table 1. Meteorological parameters and concentrations of gaseous pollutants and chemical components of PM<sub>2.5</sub> in Beijing during the 2014 APEC campaign

|   | Whole period<br>(N=48) | Before-APEC<br>(08/10–02/11)<br>(N=26) | During-APE<br>(03/11–12/11)<br>(N=10) | After-APEC<br>(13/11–14/11)<br>(N=12) |
|---|------------------------|--|---------------------------------------|---------------------------------------|
| I. Meteorological parameters                                    |                        |  |                                       |                                       |
| Temperature, °C   | 9.5±4.3 (3.0–18)       | 13±2.6 (9.0–18)                        | 7.0±1.7 (4.0–10)                      | 4.3±1.3 (3.0–7.0)                     |
| Relative humidity,  | 56±19 (17–88)          | 62±19 (22–88)                          | 47±14 (17–65)                         | 51±16 (29–80)                         |
| Visibility, km  | 8.8±6.8 (1.0–28)       | 7.3±6.6 (1.0–24)                       | 13±7.7 (6.0–28)                       | 7.2±4.2 (2.0–15)                      |
| Wind speed, km h <sup>-1</sup>                                  | 8.0±4.9 (3.0–26)       | 7.6±4.8 (3.0–26)                       | 9.4±6.6 (3.0–26)                      | 7.8±2.9 (3.0–13)                      |
| II. Gaseous pollutants, µg m <sup>-3</sup>                      |                        |  |                                       |                                       |
| O <sub>3</sub>  | 48 ± 23 (6.0–115)      | 55 ± 24 (9.0–115)                      | 52 ± 13 (25–69)                       | 29 ± 18 (6.0–60)                      |
| SO <sub>2</sub>   | 12 ± 8.5 (2.0–43)      | 8.8 ± 4.6 (2.0–19)                     | 7.6 ± 3.9 (2.0–15)                    | 23 ± 8.8 (13–43)                      |
| NO <sub>2</sub>   | 68 ± 29 (10–135)       | 71 ± 27 (22–118)                       | 45 ± 18 (10–69)                       | 78 ± 29 (45–135)                      |
| CO  | 1360 ± 730 (220–3320)  | 1370 ± 700 (250–2460)                  | 960 ± 410 (220–1420)                  | 1720 ± 830 (740–3320)                 |
| III. Major components of PM <sub>2.5</sub> , µg m <sup>-3</sup> |                        |  |                                       |                                       |
| PM <sub>2.5</sub>   | 157 ± 110 (16–408)     | 178 ± 122 (16–408)                     | 98 ± 46 (28–183)                      | 161 ± 100 (36–383)                    |
| SO <sub>4</sub> <sup>2-</sup>                                   | 12 ± 11.5 (1.2–43)     | 15 ± 13 (1.2–43)                       | 5.3 ± 2.8 (1.8–11)                    | 11 ± 10 (2.9–34)                      |
| NO <sub>3</sub> <sup>-</sup>                                    | 21 ± 22 (0.32–88)      | 28 ± 26 (0.32–88)                      | 10 ± 8.1 (1.2–26)                     | 15 ± 13 (2.9–46)                      |
| NH <sub>4</sub> <sup>+</sup>                                    | 7.3 ± 7.2 (0.2–28)     | 9.0 ± 8.0 (0.2–28)                     | 3.1 ± 2.6 (0.2–8.6)                   | 6.9 ± 6.4 (1.0–22)                    |
| OC  | 28 ± 18 (5.7–78)       | 26 ± 16 (6.0–67)                       | 19 ± 7.6 (5.7–29)                     | 39 ± 23 (9.7–78)                      |
| EC  | 8.8 ± 5.4 (1.4–25)     | 8.6 ± 4.6 (1.4–18)                     | 6.0 ± 2.7 (1.5–9.6)                   | 12 ± 7.0 (2.1–25)                     |
| WSOC  | 10 ± 6.0 (2.4–32)      | 11 ± 4.6 (3.1–32)                      | 6.4 ± 2.6 (2.4–11)                    | 11 ± 6.1 (4.5–24)                     |
| ALWC  | 40 ± 62 (0–299)        | 58 ± 75 (0–299)                        | 6.3 ± 5.5 (0–19)                      | 28 ± 41 (0.4–136)                     |
| [H <sup>+</sup> ]   | 0.083 ± 0.14 (0–0.56)  | 0.13 ± 0.17 (0–0.56)                   | 0.026 ± 0.025 (0–0.072)               | 0.033 ± 0.067 (0–0.20)                |

Table 2. Concentrations of dicarboxylic acids and related compounds in PM<sub>2.5</sub> in Beijing during the 2014 APEC campaign (ng m<sup>-3</sup>)

|                                 | Whole period<br>(N=48) | Before-APEC<br>(08/10–02/11)<br>(N=26) | During-APE<br>(03/11–12/11)<br>(N=10) | After-APEC<br>(13/11–14/11)<br>(N=12) |
|---------------------------------|------------------------|--|---------------------------------------|---------------------------------------|
| I. Dicarboxylic acids           |                        |  |                                       |                                       |
| Oxalic, C <sub>2</sub>          | 334 ± 461 (10–2127)    | 502 ± 564 (10.5–2127)                  | 101 ± 69 (35–251)                     | 166 ± 157 (22–554)                    |
| Malonic, C <sub>3</sub>         | 31 ± 42 (ND–247)       | 45.7 ± 52.1 (1.44–247)                 | 12 ± 8.0 (3.4–22.8)                   | 16 ± 10.9 (ND–36)                     |
| Succinic, C <sub>4</sub>        | 74 ± 118 (3.0–722)     | 111 ± 150 (3.0–722)                    | 24 ± 14 (7.1–42)                      | 36 ± 26 (4.9–90)                      |
| Glutaric, C <sub>5</sub>        | 8.7 ± 12 (ND–68)       | 13 ± 15 (ND–68.1)                      | 2.9 ± 2.24 (0.9–5.8)                  | 4.9 ± 4.2 (ND–13)                     |
| Adipic, C <sub>6</sub>          | 13 ± 14 (0.9–83)       | 17 ± 18 (1.9–83)                       | 5.9 ± 3.8 (2.1–14)                    | 9.9 ± 7.1 (2.0–23)                    |
| Pimelic, C <sub>7</sub>         | 2.1 ± 3.8 (ND–27)      | 2.6 ± 5.1 (ND–27)                      | 1.1 ± 0.7 (0.2–2.3)                   | 2.0 ± 1.1 (0.9–4.4)                   |
| Suberic, C <sub>8</sub>         | 10 ± 11 (ND–66)        | 12 ± 13 (ND–66)                        | 7.6 ± 5.0 (1.3–16)                    | 8.7 ± 6.0 (2.0–21)                    |
| Azelaic, C <sub>9</sub>         | 5.0 ± 4.9 (0.5–21)     | 6.4 ± 5.7 (0.6–21)                     | 1.7 ± 0.9 (0.5–3.2)                   | 4.6 ± 3.3 (1.3–13)                    |
| Sebacic, C <sub>10</sub>        | 7.7 ± 7.4 (ND–34)      | 9.4 ± 8.8 (ND–34)                      | 4.2 ± 3.6 (0.5–11)                    | 6.8 ± 4.9 (1.4–16)                    |
| Undecanedioic, C <sub>11</sub>  | 11 ± 13 (ND–77)        | 14 ± 16 (ND–77)                        | 3.3 ± 2.5 (ND–7.5)                    | 9.4 ± 6.4 (0.8–23)                    |
| Methylsuccinic, iC <sub>5</sub> | 13 ± 16 (0.6–79)       | 18 ± 19 (0.6–79)                       | 4.8 ± 3.0 (1.0–9.2)                   | 8.4 ± 6.0 (2.3–19)                    |
| Methylglutaric, iC <sub>6</sub> | 7.5 ± 10 (ND–36)       | 11 ± 12 (ND–36)                        | 0.9 ± 0.9 (ND–2.6)                    | 4.6 ± 5.1 (ND–14)                     |
| Maleic, M                       | 3.4 ± 3.9 (ND–15)      | 4.6 ± 4.7 (ND–15)                      | 1.4 ± 0.8 (ND–2.9)                    | 2.4 ± 2.0 (ND–6.3)                    |
| Fumaric, F                      | 7.2 ± 8.8 (ND–64)      | 10 ± 11 (ND–64)                        | 2.2 ± 1.5 (ND–5.4)                    | 4.7 ± 3.2 (1.4–10)                    |
| Phthalic, Ph                    | 17 ± 14 (1.5–64)       | 20 ± 16 (1.5–64)                       | 10 ± 6.8 (2.3–20)                     | 17 ± 9.0 (6.4–31)                     |
| Isophthalic, iPh                | 2.1 ± 2.5 (ND–10)      | 2.9 ± 2.8 (ND–10)                      | 2.0 ± 2.1 (0.2–5.9)                   | 0.5 ± 0.3 (ND–3.2)                    |
| Terephthalic, tPh               | 46 ± 35 (2.6–133)      | 50 ± 35 (2.6–123)                      | 28 ± 19 (4.7–59)                      | 53 ± 40 (7.4–133)                     |
| Subtotal                        | 593 ± 739 (25–3788)    | 849 ± 905 (25–3788)                    | 214 ± 135 (72–447)                    | 354 ± 279 (85–965)                    |
| II. Keto-carboxylic acids       |                        |  |                                       |                                       |
| Pyruvic, Pyr                    | 24 ± 20 (1.3–84)       | 31 ± 23 (2.4–84)                       | 15 ± 12 (1.3–36)                      | 15 ± 9.3 (3.2–33)                     |
| Glyoxylic, ωC <sub>2</sub>      | 33 ± 51 (1.2–300)      | 48 ± 64 (1.2–300)                      | 10 ± 7.7 (2.6–21)                     | 20 ± 23 (2.8–80)                      |
| 7-Oxoheptanoic, ωC <sub>7</sub> | 8.8 ± 14 (ND–90)       | 13 ± 17 (ND–90)                        | 4.2 ± 3.6 (ND–13)                     | 4.5 ± 5.1 (ND–17)                     |
| Subtotal                        | 66 ± 81 (3.6–474)      | 92 ± 99 (3.6–474)                      | 30 ± 22 (5.9–66)                      | 40 ± 35 (13–128)                      |
| III α-Dicarbonyls               |                        |  |                                       |                                       |
| Glyoxal, Gly                    | 44 ± 47 (4.2–270)      | 57 ± 56 (4.2–270)                      | 22 ± 19 (4.9–47)                      | 35 ± 30 (7.3–101)                     |
| Methylglyoxal, mGly             | 82 ± 82 (ND–406)       | 102 ± 96 (ND–406)                      | 60 ± 52 (15–139)                      | 58 ± 51 (5.8–144)                     |
| Subtotal                        | 126 ± 115 (5.3–466)    | 158 ± 132 (5.3–466)                    | 81.6 ± 67.4 (22–186)                  | 93 ± 80 (14–225)                      |
| TDOC <sup>b</sup>               | 785 ± 872 (36–4636)    | 1099 ± 1104 (36–4636)                  | 325 ± 220 (107–664)                   | 487 ± 387 (117–1318)                  |

<sup>a</sup>ND: not detectable; <sup>b</sup>TDOC: total detected organic compounds.

593  
594  
595  
596

Table 3 Linear correlation coefficients of  $\delta^{13}\text{C}$  of  $\text{C}_2$  with  $\text{C}_2/\omega\text{C}_2$ ,  $\text{C}_2/\text{mGly}$ , and TDOC/WSOC

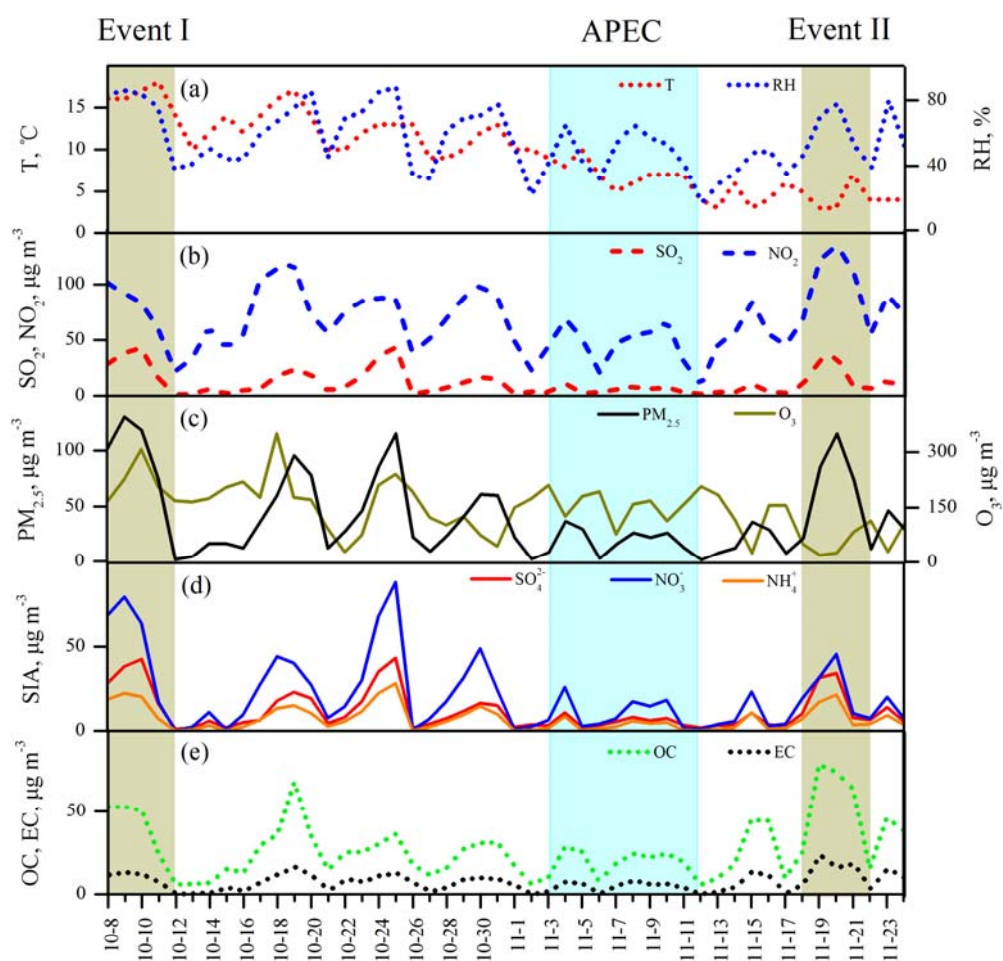
|                       | $\text{C}_2/\omega\text{C}_2$ | $\text{C}_2/\text{mGly}$ | TDOC/WSOC |
|-----------------------|-------------------------------|--------------------------|-----------|
| $\delta^{13}\text{C}$ | 0.49**                        | 0.35*                    | 0.41*     |

\*\*  $p < 0.01$ ; \*  $p < 0.05$

Table 4. Meteorological parameters and chemical compositions ( $\mu\text{g m}^{-3}$ ) of two maximum  $\text{PM}_{2.5}$  between two pollution episodes in Beijing

|                                       | T ( $^{\circ}\text{C}$ ) | RH (%)      | V <sup>a</sup> (km) | $\text{PM}_{2.5}$ | OC          | EC         | SIA <sup>b</sup> | TDOC <sup>c</sup> |
|---------------------------------------|--------------------------|-------------|---------------------|-------------------|-------------|------------|------------------|-------------------|
| Event I<br>(8/10-11/10, Before-APEC)  | $16.7 \pm 0.8$           | $82 \pm 4$  | $1.5 \pm 0.5$       | $349 \pm 57$      | $45 \pm 12$ | $12 \pm 2$ | $106 \pm 39$     | $2749 \pm 1357$   |
| Event II<br>(18/11-21/11, After-APEC) | $4.5 \pm 1.7$            | $62 \pm 13$ | $3.5 \pm 1.5$       | $259 \pm 102$     | $60 \pm 21$ | $17 \pm 6$ | $60 \pm 32$      | $831 \pm 400$     |

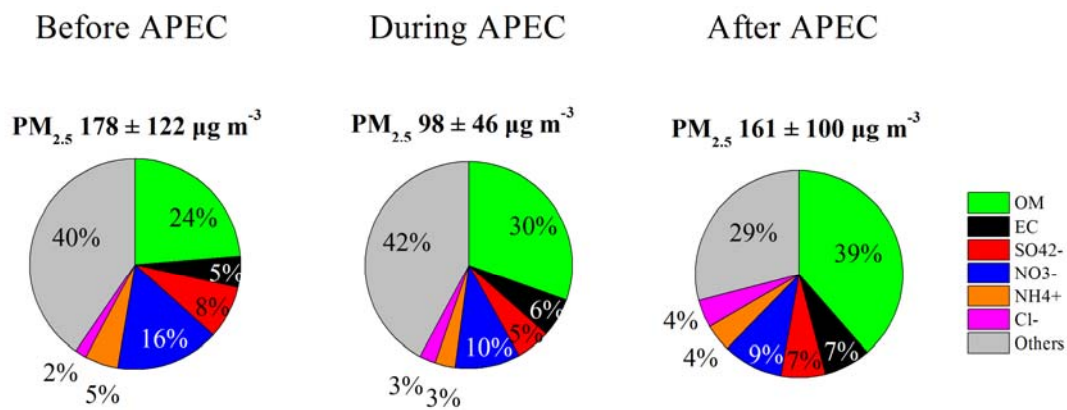
<sup>a</sup>V: visibility; <sup>b</sup>SIA: secondary inorganic ions (the sum of sulfate, nitrate and ammonium); <sup>c</sup>TDOC: total detected organic compounds



600

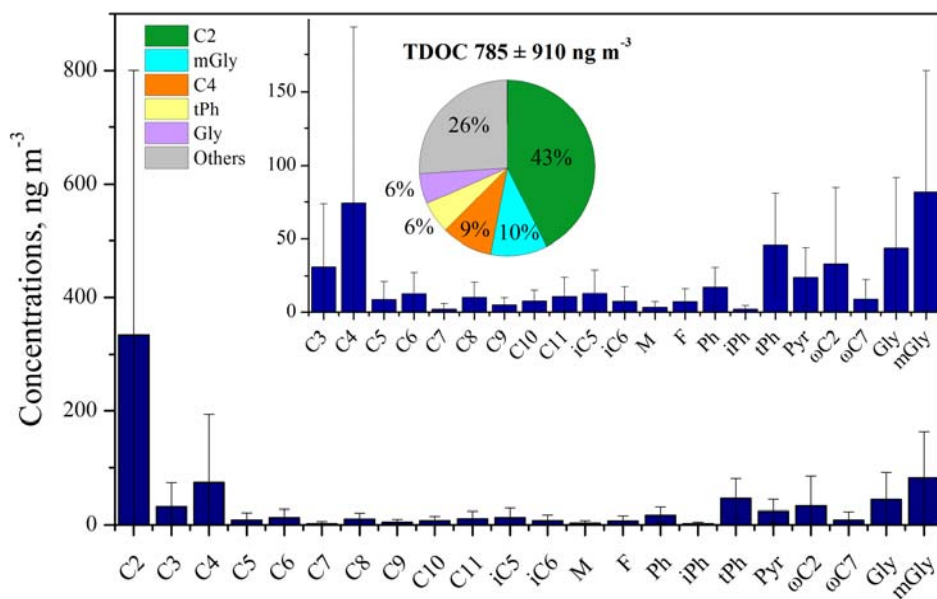
601 **Figure 1.** Temporal variations of meteorological conditions, gaseous pollutants and major components of  $PM_{2.5}$   
 602 during the 2014 APEC campaign. (The brown shadows represent two air pollution events characterized  
 603 by highest  $PM_{2.5}$  levels before- and after-APEC, while the blue shadow represents the APEC event).





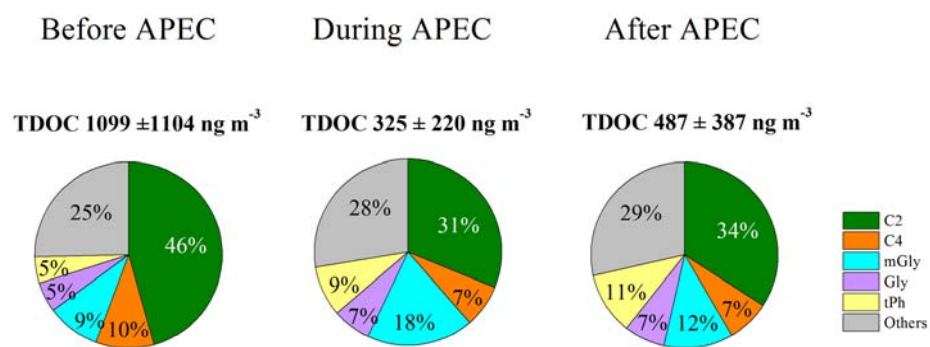
604  
605  
606

**Figure 2.** Chemical composition of  $PM_{2.5}$  during the 2014 APEC campaign.



608

609 **Figure 3.** Molecular distributions of dicarboxylic acids and related compounds in  $\text{PM}_{2.5}$  of Beijing, China during the  
 610 2014 APEC campaign. The pie chart is the average composition of total detected organic compounds  
 611 (TDOC) and the top number is the average mass concentration of TDOC of the whole study period.  
 612

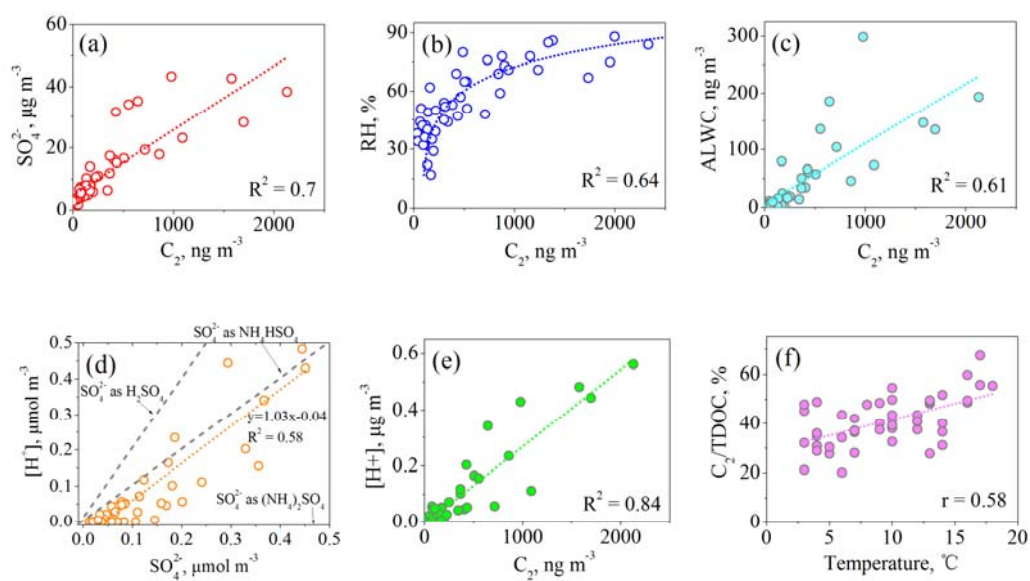


614

615

**Figure 4.** Compositions of total detected organic compounds (TDOC) in PM<sub>2.5</sub> during the 2014 APEC campaign.

616



618

619 **Figure 5.** Correlation analysis for oxalic acid ( $C_2$ ) and sulfate in  $PM_{2.5}$  during the whole 2014 APEC campaign. (a-c)620 Concentrations of  $C_2$  with sulfate, relative humidity (RH), and aerosol liquid water content (ALWC); (d, e)621 sulfate and  $C_2$  with aerosol acidity  $[H^+]$  and (f) temperature with mass ratio of  $C_2$  to total detected organic622 compounds ( $C_2/TDOC$ ).

623

624

625

626

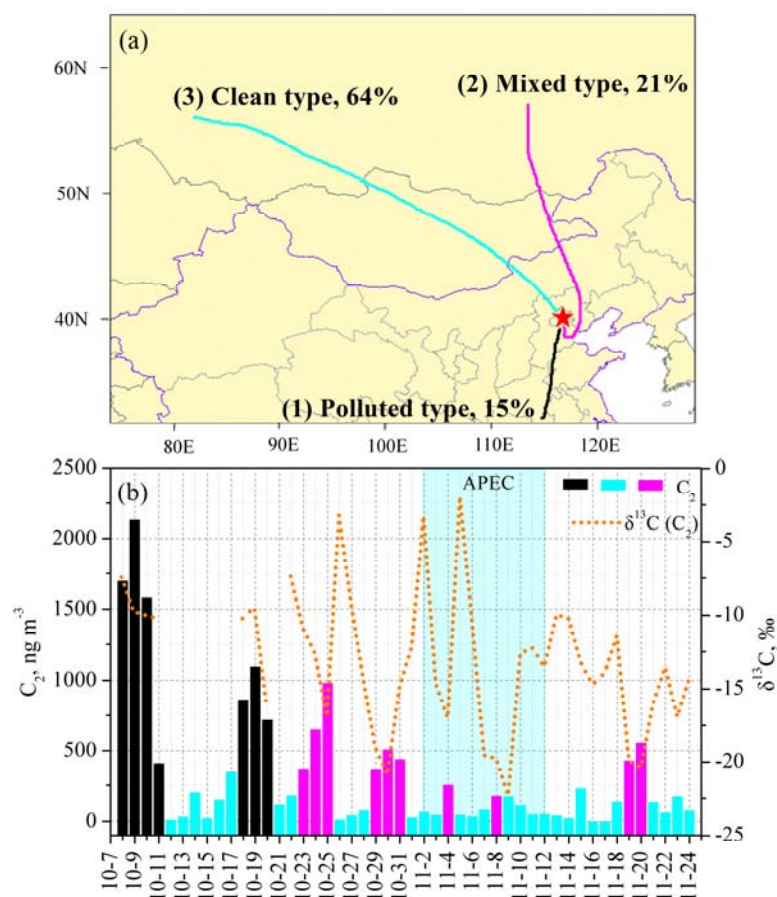
627

628

629

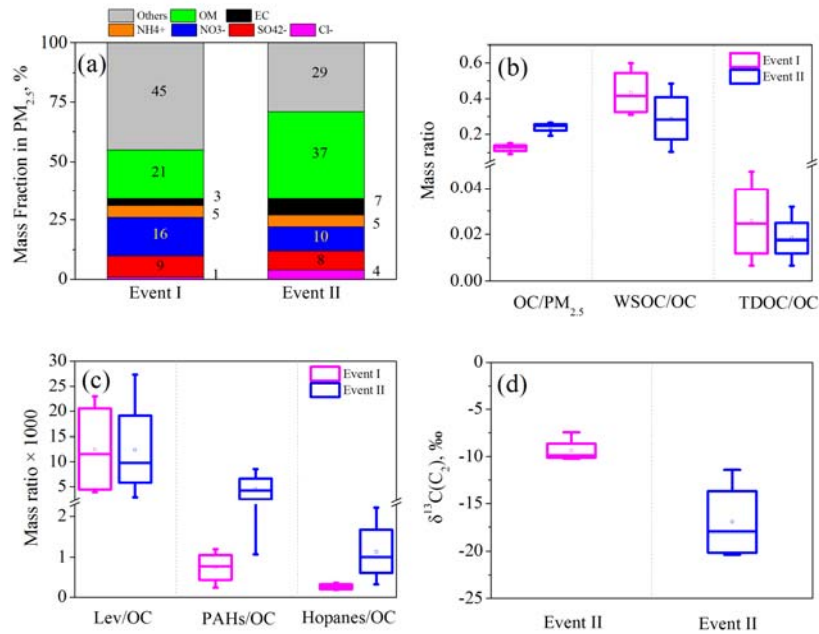
630

631



632  
 633 **Figure 6.** (a) 72-h backward trajectories determined by the National Oceanic and Atmospheric Administration  
 634 Hybrid Single Particle Lagrangian Integrated Trajectory (HYSPLIT) model arriving at the sampling site to  
 635 reveal the major air mass flow types during the study period. Northwestern wind (light blue) was most  
 636 frequently (64%), followed by northerly (21%, pink) and southerly (15%, black) and is defined as clean,  
 637 mixed and polluted types, respectively (see the definitions in the text); (b) Time series of  $\delta^{13}\text{C}$  values and  
 638 concentration of oxalic acid during the whole study period (Colors in Fig. 6a are corresponding to those in  
 639 Fig. 6b).

640  
 641  
 642  
 643  
 644  
 645  
 646



647  
 648 **Figure 7.** Comparison of chemical composition of PM<sub>2.5</sub> during two air pollution events. **(a)** Percentages of major  
 649 species in PM<sub>2.5</sub>; **(b, c)** mass ratios of major species and organic tracers in PM<sub>2.5</sub>; **(d)** stable carbon  
 650 isotope composition of oxalic acid (C<sub>2</sub>) (Data about levoglucosan (Lev), PAHs and hopanes are cited  
 651 from Wang et al (2016)).  
 652